ELSEVIER

0266-3538(95)00105-0

Composites Science and Technology **55** (1995) 277–285

0266-3538/95/$09.50

BUCKLING OPTIMIZATION OF SYMMETRICALLY LAMINATED PLATES WITH VARIOUS GEOMETRIES AND END CONDITIONS

Hsuan-Teh Hu & Bor-Horng Lin

Department of Civil Engineering, National Cheng Kung University, 1 University Road, Tainan 701, Taiwan

(Received 17 March 1995; revised version received 26 May 1995; accepted 31 July 1995)

Abstract

The buckling resistance of symmetrically laminated plates with a given material system and subjected to uniaxial compression is maximized with respect to fiber orientations by using a sequential linear programming method together with a simple move-limit strategy. Significant influence of plate thicknesses, aspect ratios, central circular cutouts and end conditions on the optimal fiber orientations and the associated optimal buckling loads of symmetrically laminated plates are shown.

Keywords: buckling, optimization, symmetrically laminated plates, end conditions, sequential linear programming

1 INTRODUCTION

The use of fiber-reinforced laminated composite plates in aerospace structures has increased rapidly in recent years. The composite plates in service are commonly subjected to various kinds of compression which may cause buckling. Hence, structural instability becomes a major concern in safe and reliable design of the composite plates. The buckling resistance of composite laminate plates depends on end conditions, lamination parameters such as ply orientations,[1–4] and geometric variables such as aspect ratios, thicknesses and cutouts.[3,5–8] Therefore, for composite plates with a given material system, geometric shape, thickness and end condition, the proper selection of appropriate lamination to achieve maximum buckling resistance becomes a crucial problem.

Research on the subject of structural optimization has been reported previously.[9] Among various optimization schemes, the method of sequential linear programming has been successfully applied to many large-scale structural problems.[10,11] Hence, linearization of non-linear optimization problems to meet requirements for iterative applications of a linear programming method is one of the most popular approaches to solving the structural optimization problem.

In the present investigation, buckling optimization of symmetrically laminated plates with respect to fiber orientations is performed by using a sequential linear programming method together with a simple move-limit strategy. The critical buckling loads of composite plates are calculated by the bifurcation buckling analysis implemented in the ABAQUS finite element program.[12] In the present paper, the bifurcation buckling analysis, the constitutive equations for fiber-composite laminate and the optimization method are briefly reviewed first. Then the influence of end conditions, plate thicknesses, aspect ratios, and cutouts on the optimal fiber orientations and the associated optimal buckling loads of composite plates is presented. Finally, important conclusions obtained from this study are given.

2 BIFURCATION BUCKLING ANALYSIS

In the finite element analysis, a system of non-linear algebraic equations results in the incremental form:

$$[K_t]\mathrm{d}\{u\} = \mathrm{d}\{p\} \tag{1}$$

where $[K_t]$ is the tangent stiffness matrix, $\mathrm{d}\{u\}$ the incremental nodal displacement vector and $\mathrm{d}\{p\}$ the incremental nodal force vector.

Within the range of elastic behavior, it is known that when the deformation of a structure is small, the non-linear theory leads to the same critical load as the linear theory.[13,14] Consequently, if only the buckling load is to be determined, the calculation can be greatly simplified by assuming the deformation to be small and we can neglect the non-linear terms which are functions of nodal displacements in the tangent stiffness matrix. The linearized formulation then gives

rise to a tangent stiffness matrix in the following expression:[15]

$$[K_t] = [K_L] + [K_\sigma] \tag{2}$$

where $[K_L]$ is a linear stiffness matrix and $[K_\sigma]$ a stress stiffness matrix. If a stress stiffness matrix $[K_\sigma]_{ref}$ is generated according to a reference load $\{p\}_{ref}$, for another load level $\{p\}$ (with λ being a scalar multiplier), we have:

$$\{p\} = \lambda\{p\}_{ref}; \quad [K_\sigma] = \lambda[K_\sigma]_{ref} \tag{3}$$

When buckling occurs, the external loads do not change, i.e. $d\{p\} = 0$. Then the bifurcation solution for the linearized buckling problem may be determined from the following eigenvalue equation:

$$([K_L] + \lambda_{cr}[K_\sigma]_{ref})d\{u\} = 0 \tag{4}$$

where λ_{cr} is an eigenvalue and $d\{u\}$ becomes the eigenvector defining the buckling mode. The critical load $\{p\}_{cr}$ can be obtained from $\{p\}_{cr} = \lambda_{cr}\{p\}_{ref}$. In ABAQUS, a subspace iteration procedure[16] is used to solve for the eigenvalues and eigenvectors.

3 CONSTITUTIVE MATRIX FOR FIBER-COMPOSITE LAMINAE

In finite element analysis, the laminate plates are modeled by eight-node isoparametric laminate shell elements with six degrees of freedom per node (three displacements and three rotations). The formulation of the shell allows transverse shear deformation.[12,17] These shear flexible shells can be used for both thick and thin shell applications.[12]

During the analysis, the constitutive matrices of composite materials at element integration points must be calculated before the stiffness matrices are assembled from element level to global level. For fiber-composite laminate materials, each lamina can be considered as an orthotropic layer. The stress/strain relationships for a lamina in the material coordinates (1,2,3) (Fig. 1) at an element integration point can be written as:

$$\{\sigma'\} = [Q_1]\{\epsilon'\};$$

$$[Q_1'] = \begin{bmatrix} \dfrac{E_{11}}{1-\nu_{12}\nu_{21}} & \dfrac{\nu_{12}E_{22}}{1-\nu_{12}\nu_{21}} & 0 \\ \dfrac{\nu_{21}E_{11}}{1-\nu_{12}\nu_{21}} & \dfrac{E_{22}}{1-\nu_{12}\nu_{21}} & 0 \\ 0 & 0 & G_{12} \end{bmatrix} \tag{5}$$

$$\{\tau'\} = [Q_2']\{\gamma'\}; \quad [Q_2'] = \begin{bmatrix} \alpha_1 G_{13} & 0 \\ 0 & \alpha_2 G_{23} \end{bmatrix} \tag{6}$$

where $\{\sigma'\} = \{\sigma_1, \sigma_2, \tau_{12}\}^T$, $\{\tau'\} = \{\tau_{13}, \tau_{23}\}^T$, $\{\epsilon'\} = \{\epsilon_1, \epsilon_2, \gamma_{12}\}^T$, $\{\gamma'\} = \{\gamma_{13}, \gamma_{23}\}^T$, and α_1 and α_2 are shear correction factors. In ABAQUS, the shear correction factors are calculated by assuming that the transverse shear energy through the thickness of the laminate is equal to that of the case of unidirectional bending.[12,18]

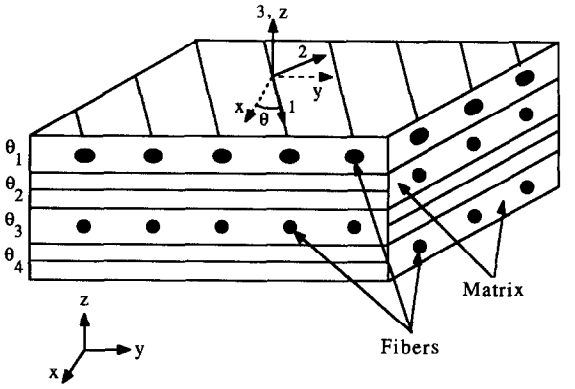

Fig. 1. Material and element coordinate systems for fiber-composite laminate.

The constitutive equations for the lamina in the element coordinates (x,y,z) then become:

$$\{\sigma\} = [Q_1]\{\epsilon\}; \quad [Q_1] = [T_1]^T[Q_1'][T_1] \tag{7}$$

$$\tau = [Q_2]\{\gamma\}; \quad [Q_2] = [T_2]^T[Q_2'][T_2] \tag{8}$$

$$[T_1] = \begin{bmatrix} \cos^2\theta & \sin^2\theta & \sin\theta\cos\theta \\ \sin^2\theta & \cos^2\theta & -\sin\theta\cos\theta \\ -2\sin\theta\cos\theta & 2\sin\theta\cos\theta & \cos^2\theta - \sin^2\theta \end{bmatrix} \tag{9}$$

$$[T_2] = \begin{bmatrix} \cos\theta & \sin\theta \\ -\sin\theta & \cos\theta \end{bmatrix} \tag{10}$$

where $\{\sigma\} = \{\sigma_x, \sigma_y, \sigma_{xy}\}^T$, $\{\tau\} = \{\tau_{xz}, \tau_{yz}\}^T$, $\{\epsilon\} = \{\epsilon_x, \epsilon_y, \gamma_{xy}\}^T$, $\{\gamma\} = \{\gamma_{xz}, \gamma_{yz}\}^T$, and the fiber orientation, θ, is measured counterclockwise from the element local x axis to the material 1 axis.

Let $\{\epsilon_o\} = \{\epsilon_{xo}, \epsilon_{yo}, \gamma_{xyo}\}^T$ be the in-plane strains at the mid-surface of the laminate section, $\{\kappa\} = \{\kappa_x, \kappa_y, \kappa_{xy}\}^T$ the curvatures, and h the total thickness of the section. If there are n layers in the layup, the stress resultants, $\{N\} = \{N_x, N_y, N_{xy}\}^T$, $\{M\} = \{M_x, M_y, M_{xy}\}^T$ and $\{V\} = \{V_x, V_y\}^T$, can be defined as:

$$\begin{Bmatrix} \{N\} \\ \{M\} \\ \{V\} \end{Bmatrix} = \int_{-h/2}^{h/2} \begin{Bmatrix} \{\sigma\} \\ z\{\sigma\} \\ \{\tau\} \end{Bmatrix} dz = \int_{-h/2}^{h/2} \begin{Bmatrix} [Q_1]\{\epsilon\} \\ z[Q_1]\{\epsilon\} \\ [Q_2]\{\gamma\} \end{Bmatrix} dz$$

$$= \int_{-h/2}^{h/2} \begin{Bmatrix} [Q_1](\{\epsilon_0\} + z\{\kappa\}) \\ z[Q_1](\{\epsilon_0\} + z\{\kappa\}) \\ [Q_2]\{\gamma\} \end{Bmatrix} dz$$

$$= \sum_{j=1}^{n} \begin{bmatrix} (z_{jt} - z_{jb})[Q_1] & \frac{1}{2}(z_{jt}^2 - z_{jb}^2)[Q_1] & [0] \\ \frac{1}{2}(z_{jt}^2 - z_{jb}^2)[Q_1] & \frac{1}{3}(z_{jt}^3 - z_{jb}^3)[Q_1] & [0] \\ [0]^T & [0]^T & (z_{jt} - z_{jb})[Q_2] \end{bmatrix} \begin{Bmatrix} \{\epsilon_0\} \\ \{\kappa\} \\ \{\gamma\} \end{Bmatrix} \tag{11}$$

where z_{jt} and z_{jb} are the distance from the mid-surface of the section to the top and the bottom of the jth

layer respectively. [0] represents a 3 by 2 matrix with all the coefficients equal to zero. It can be noted that for composite laminae with symmetric layup, the extensional and the flexural terms in eqn (11) become uncoupled, i.e.

$$\sum_{j=1}^{n} \frac{1}{2}(z_{jt}^2 - z_{jb}^2)[Q_1] = \begin{bmatrix} 0 & 0 & 0 \\ 0 & 0 & 0 \\ 0 & 0 & 0 \end{bmatrix} \tag{12}$$

4 SEQUENTIAL LINEAR PROGRAMMING

A general optimization problem may be defined as: minimize

$$f(\underline{x}) \tag{13a}$$

subject to:

$$g_i(\underline{x}) \leq 0, \quad i = 1, \ldots, r \tag{13b}$$

$$h_j(\underline{x}) = 0, \quad j = r+1, \ldots, m \tag{13c}$$

$$p_k \leq x_k \leq q_k, \quad k = 1, \ldots, n \tag{13d}$$

where $\underline{x} = \{x_1, x_2, \ldots, x_n\}^T$ is a vector of design variables, $f(\underline{x})$ is an objective function, $g_i(\underline{x})$ are inequality constraints, and $h_j(\underline{x})$ are equality constraints. p_k and q_k are lower and upper limits of the variable x_k. If an optimization problem requires maximization, we simply minimize $-f(\underline{x})$.

For the optimization problem of eqns (13), a linearized problem may be constructed by approximating the non-linear functions at a current solution point, $\underline{x}_o = (x_{o1}, x_{o2}, \ldots, x_{on}\}^T$, in a first-order Taylor series expansion as follows: minimize

$$f(\underline{x}) \approx f(\underline{x}_o) + \nabla f(\underline{x}_o)^T \delta\underline{x} \tag{14a}$$

subject to:

$$g_i(\underline{x}) \approx g_i(\underline{x}_o) + \nabla g_i(\underline{x}_o)^T \delta\underline{x} \leq 0 \tag{14b}$$

$$h_j(\underline{x}) \approx h_j(\underline{x}_o) + \nabla h_j(\underline{x}_o)^T \delta\underline{x} = 0 \tag{14c}$$

$$p_k \leq x_k \leq q_k \tag{14d}$$

where $i = 1, \ldots, r$; $j = r+1, \ldots, m$; $k = 1, \ldots, n$; $\delta\underline{x} = \{x_1 - x_{o1}, x_2 - x_{o2}, \ldots, x_n - x_{on}\}^T$.

It is clear that eqns (14) represent a linear programming problem and a solution for these equations may be easily obtained by the simplex method.[19] After obtaining an initial approximate solution for eqns (14), say $\underline{x}_1$, we can linearize the original problem, eqns (13), at $\underline{x}_1$ and solve the new linear programming problem. The process is repeated until a precise solution is achieved. This approach is referred to as sequential linear programming.[10,11]

Although the procedure for sequential linear programming is simple, the optimum solution for the approximated linear problem may violate the constraint conditions of the original optimization problem. In addition, if the true optimum solution of a non-linear problem appears between two constraint intersections, a straightforward successive linearization may lead to an oscillation of the solution between the widely separated values. Difficulties in dealing with such problems may be avoided by imposing a 'move limit'[10,11] on the linear approximation, which is a set of box-like admissible constraints placed on the range of $\delta\underline{x}$. Generally, the choice of a proper move limit depends on experience and on the results of previous steps. In addition, the move limit should gradually approach zero as the iterative process of the sequential linear programming continues.[10,11,20]

The algorithm of the sequential linear programming with selected move limits may be summarized as follows:

1. linearize the non-linear objective function and associated constraints with respect to an initial guess $\underline{x}_o$;
2. impose move limits in the form of $-\underline{a} \leq (\underline{x} - \underline{x}_o) \leq \underline{b}$, where $\underline{a}$ and $\underline{b}$ are properly chosen lower and upper bounds;
3. solve the approximate linear programming problem to obtain an optimum solution $\underline{x}_1$;
4. repeat the procedures (1)–(3) by redefining $\underline{x}_1$ with $\underline{x}_o$ until either the subsequent solutions do not change significantly (i.e. true convergence) or the move limit approaches zero (i.e. forced convergence); if the solution obtained is due to forced convergence, the procedures (1)–(4) should be repeated with another initial guess.

A detailed 'flow diagram' of sequential linear programming can be found elswhere.[11]

5 RESULTS OF THE OPTIMIZATION ANALYSIS

5.1 Rectangular laminate plates with various aspect ratios and end conditions

In this section composite laminate rectangular plates subjected to a uniaxial compressive load N_x per unit length applied at the edges normal to the x direction are analyzed (Fig. 2). The width of the plates, b, is 10 cm and the length of the plates, a, is varied between 5 and 40 cm. Three types of end conditions are considered, which are two ends simply supported (denoted by S) and two ends fixed (denoted by F), four ends simply supported, and four ends fixed. These end conditions prevent out of plane displacement, w, but allow in-plane movements, u and v. In addition, all the points on the right edge of the plates are enforced to displace the same amount u in the x direction, and all the points on the upper edge of the plates are enforced to displace the same amount v in the y direction. The thickness of each ply is 0·125 mm. The laminate layups of the plates are $[\pm\theta/90/0]_{ns}$. In order to study the influence of plate thickness on the results of optimization, $n = 2$ (16-ply thin plate) and

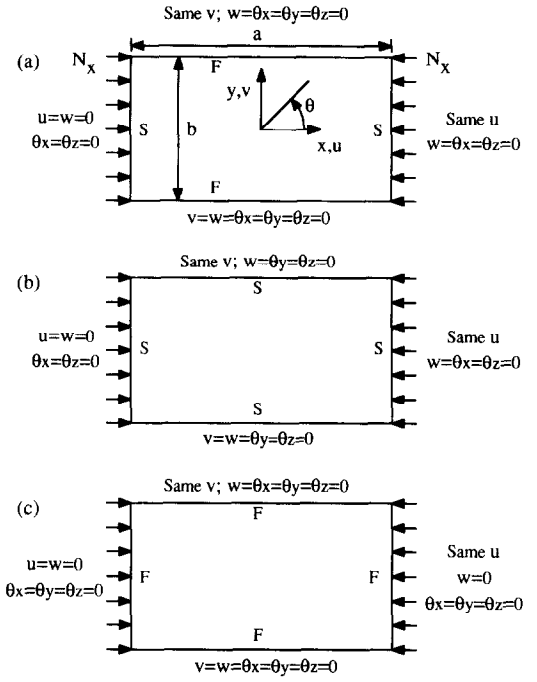

Fig. 2. Uniaxially compressed composite plates with: (a) two simply supported ends and two fixed ends; (b) four simply supported ends; and (c) four fixed ends. (F, fixed; S, simply supported.)

10 (80-ply thick plate) are selected for analysis. The lamina consists of graphite/epoxy (Hercules AS/3501-6) and material constitutive properties are taken from a previous studty:[21] $E_{11} = 128$ GPa, $E_{22} = 11$ GPa, $\nu_{12} = 0{\cdot}25$, $G_{12} = G_{13} = 4{\cdot}48$ GPa, and $G_{23} = 1{\cdot}53$ GPa. In the finite element analysis, no symmetry simplifications are made. A typical buckling mode for $[\pm 40/90/0]_{2s}$ rectangular laminate plate with $a/b = 2$ and with two simply supported ends and two fixed ends is shown in Fig. 3(a).

Based on the sequential linear programming method, in each iteration the current linearized optimization problem becomes: maximize

$$N_{xcr}(\theta) \approx N_{xcr}(\theta_o) + (\theta - \theta_o)\left.\frac{\partial N_{xcr}}{\partial \theta}\right|_{\theta=\theta_o} \tag{15a}$$

subject to:

$$0° \le \theta \le 90° \tag{15b}$$

$$-r \times q \times 0{\cdot}5^s \le (\theta - \theta_o) \le r \times q \times 0{\cdot}5^s \tag{15c}$$

where N_{xcr} is the critical buckling load, θ_o is a solution obtained in the previous iteration, and r and q are the size and the reduction rate of the move limit. In the present study, the values of r and q are selected to be 20° and $0{\cdot}9^{(N-1)}$, where N is a current iteration number. In order to control the oscillation of the solution, a parameter $0{\cdot}5^s$ is introduced in the move limit, where s is the number of oscillations of the derivative $\partial N_{xcr}/\partial\theta$ that has taken place before the current iteration. The value of s increases by 1 if the sign of $\partial N_{xcr}/\partial\theta$ changes. Whenever oscillation of the solution occurs, the range of the move limit is reduced to half of its current value, which is similar to a bisection method.[22] This increases the solution convergent rate very rapidly.

The $\partial N_{xcr}/\partial\theta$ term in eqn (15a) may be approximated by using a forward finite-difference method with the following form:

$$\frac{\partial N_{xcr}}{\partial \theta} \approx \frac{[N_{xcr}(\theta_o + \Delta\theta) - N_{xcr}(\theta_o)]}{\Delta\theta} \tag{16}$$

Hence, to determine the value of $\partial N_{xcr}/\partial\theta$ numerically, two bifurication buckling analyses to compute $N_{xcr}(\theta_o)$ and $N_{xcr}(\theta_o + \Delta\theta)$ are needed in each iteration. In this study, the value of $\Delta\theta$ is selected to be 1° in most iterations.

This optimization problem involves only one design variable θ. Although, there are other simple techniques, such as polynomial interpolation and the golden section method, available for solving problems of one variable, the sequential linear programming method is still selected for the optimization. This is because the method can be extended to more variables (i.e. the angles of other plies) easily.[11]

Figure 4 shows the optimal fiber angle θ and the associated optimal buckling load N_{xcr} with respect to plate aspect ratio a/b for $[\pm\theta/90/0]_{2s}$ rectangular composite plates. From Fig. 4(a), we can see that the optimal fiber angle for plates with four simply supported ends is less sensitive to a/b than the corresponding plates with fixed ends. The optimal fiber angle shows the highest sensitivity for the plates with all four ends fixed. Nevertheless, the optimal fiber angles for plates with different end conditions seem to vary around certain values when the plate aspect ratios are increased. The results presented in Fig. 4(b) show that the effect of end conditions on the optimal buckling load are more pronounced for values of $a/b < 1$. As a/b increases, the optimal buckling loads approach constant values, and the difference in buckling load due to the difference in end conditions on the loaded edges of the plates disappears as it does for corresponding plates with a fixed value of θ. Overall, the highest buckling loads are exhibited by the plates with four fixed ends and the lowest by the plates with four simply supported ends, which is consistent with the trend exhibited by corresponding plates with a fixed value of θ.

Figure 5 shows the optimal fiber angle θ and the associated optimal buckling load versus plate aspect ratio for $[\pm\theta/90/0]_{10s}$ rectangular composite plates. Figure 5(a) shows that the optimal fiber orientation for plates with four fixed ends is not sensitive to a/b. The optimal fiber angle varies between 0° and 22° for

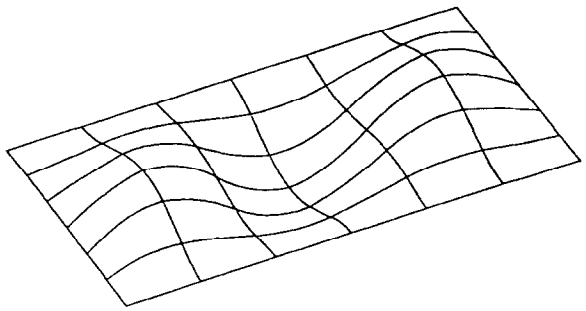

(a) Rectangular plate (a/b = 2), N_{xcr} = 2.41 kN/cm

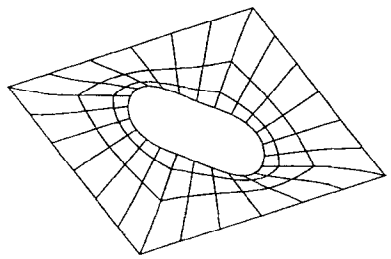

(b) Square plate (d/b = 0.5), N_{xcr} = 3.36 kN/cm

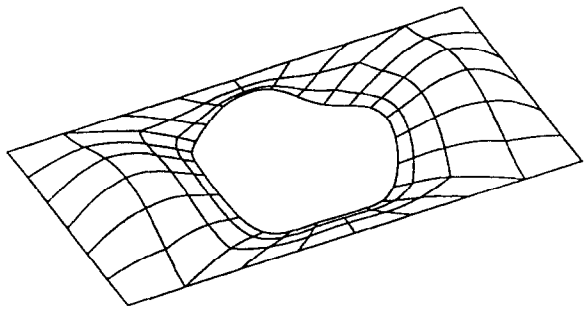

(c) Rectangular plate (a/b = 2, d/b = 0.8), N_{xcr} = 3.30 kN/cm

Fig. 3. Typical buckling modes of composite plates with $[\pm 40/90/0]_{2s}$ laminate layup and with two simply supported ends and two fixed ends.

plates with two simply supported ends and two fixed ends. For plates with four simply supported ends, the optimal fiber angle oscillates between 18° and 42°. It seems that the optimal fiber angles are sensitive to the end conditions even for large plate aspect ratios. From Fig. 5(b), it can be seen that the optimal buckling loads change significantly for plates with small aspect ratios and gradually approach constant values when the aspect ratios become large.

Comparing Fig. 5 with Fig. 4, we can observe that when the plate thicknesses are increased, not only do the optimal buckling loads of plates increase but also the transverse shear deformation greatly affects the behavioral trends of the optimal fiber angle.

5.2 Square laminate plates with various central circular cutouts and end conditions

In this section, composite laminate square plates with a central circular cutout subjected to uniaxial compressive load as shown in Fig. 6(a) are analyzed. The length of the plates, a, is 10 cm and the diameter of the cutout, d, varies between 1 and 8 cm. Three types of end conditions, i.e. SFSF, SSSS, and FFFF, similar to those in the previous section are considered. Again, the laminate layups, $[\pm\theta/90/0]_{2s}$ and $[\pm\theta/90/0]_{10s}$, are selected for analysis. A typical buckling mode for $[\pm 40/90/0]_{2s}$ square laminate plate with $d/a = 0{\cdot}5$ and with two simply supported ends and two fixed ends is shown in Fig. 3(b).

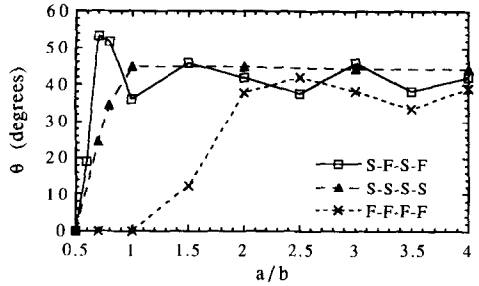

(a) Aspect ratio a/b vs. optimal fiber angle θ

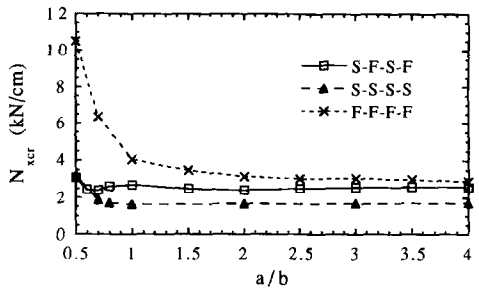

(b) Aspect ratio a/b vs. critical compressive load

Fig. 4. Effect of end conditions and plate aspect ratios on buckling optimization of uniaxially compressed $[\pm\theta/90/0]_{2s}$ rectangular composite plates.

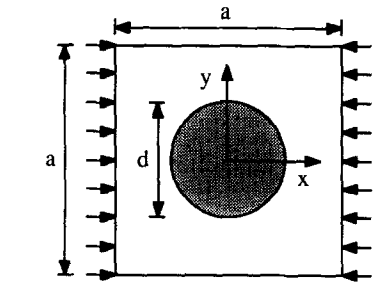

(a) Square plates

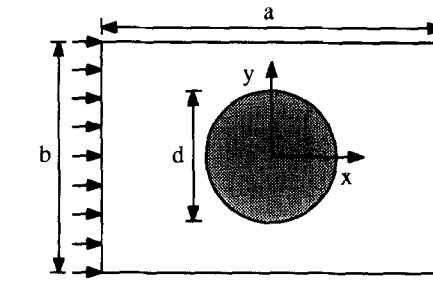

(b) Rectangular plates

Fig. 6. Composite plates with a circular cutout at center.

Figure 7 shows the optimal fiber angle and the associated optimal buckling load versus the ratio d/a for $[\pm\theta/90/0]_{2s}$ square composite plates with a central circular cutout. From Fig. 7(a), we can see that the optimal fiber orientations of these plates with various end conditions are quite different. The optimal fiber orientation shows the highest sensitivity for the plates with two simply supported ends and two fixed ends. The optimal fiber angle is around 40° for plates with four simply supported ends. For plates with four fixed

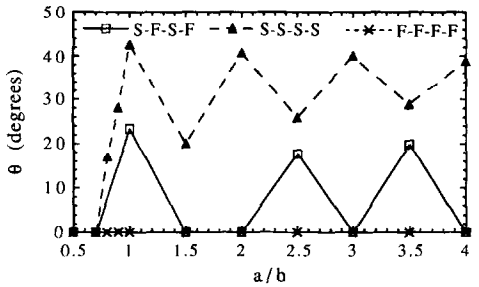

(a) Aspect ratio a/b vs. optimal fiber angle θ

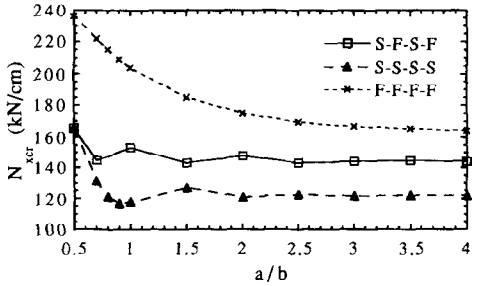

(b) Aspect ratio a/b vs. critical compressive load

Fig. 5. Effect of end conditions and plate aspect ratios on buckling optimization of uniaxially compressed $[\pm\theta/90/0]_{10s}$ rectangular composite plates.

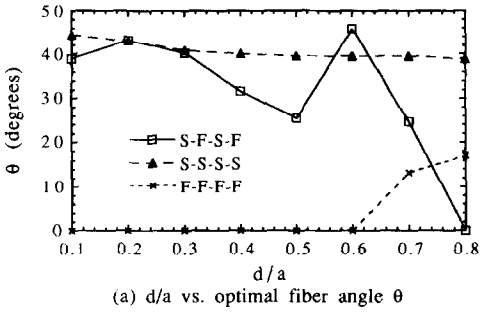

(a) d/a vs. optimal fiber angle θ

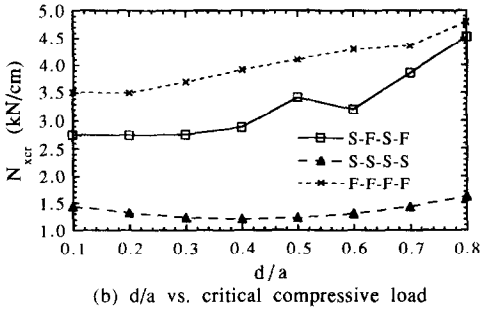

(b) d/a vs. critical compressive load

Fig. 7. Effect of end conditions and sizes of cutouts on buckling optimization of uniaxially compressed $[\pm\theta/90/0]_{2s}$ square composite plates with a central circular cutout.

ends, the optimal fiber angle is not sensitive to the sizes of the cutouts until $d/a > 0{\cdot}6$. Figure 7(b) shows that the optimal buckling loads increase with the increase of the sizes of cutouts for plates with four fixed ends, and plates with two simply supported ends and two fixed ends. This phenomenon is quite different from our intuition that introducing a large hole into a plate can cause a reduction in the buckling load of the plate. However, a previous study of isotropic plates[23] did show that introducing a hole into a plate does not always reduce the buckling load and, in some instances, may increase its buckling load. In addition, this notion has been verified both numerically and experimentally[7] for orthotropic laminated plates. For plates with four simply supported ends, the optimal buckling load first decreases then increases with increasing d/a ratio.

Figure 8 shows the optimal fiber angle and the optimal buckling load with respect to the d/a ratio for $[\pm\theta/90/0]_{10s}$ square composite plates with a central circular cutout. We can observe that the optimal fiber angles and optimal buckling loads of plates with two simply supported ends and two fixed ends are the same as those of plates with four fixed ends. We can also observe that for the same d/a ratio, the plates with four simply supported ends have the greatest optimal fiber angles and have the lowest buckling loads. However, the difference in optimal fiber angle and buckling load due to the difference in end conditions disappears when the size of the cutout is large (say $d/a > 0{\cdot}6$). In spite of the end conditions, the optimal buckling loads of these plates decrease with increasing size of cutouts.

Comparing Fig. 8 with Fig. 7, we can observe that the plate thickness has very little influence on the optimal fiber orientations of plates with four fixed ends. However, it affects significantly the optimal fiber orientations of plates with four simply supported ends and plates with two simply supported ends and two fixed ends.

5.3 Rectangular laminate plates containing a central circular cutout with various aspect ratios and end conditions

In this section composite laminate rectangular plates with a central circular cutout subjected to uniaxial compressive load as shown in Fig. 6(b) are analyzed. The width of the plates, b, is 10 cm, the length of the plates, a, varies between 5 and 40 cm, and the diameter of the cutout, d, is selected to be 8 cm. Again, three types of end conditions, SFSF, SSSS, and FFFF, and two types of laminate layups, $[\pm\theta/90/0]_{2s}$ and $[\pm\theta/90/0]_{10s}$, are selected for analysis. A typical buckling mode for $[\pm 40/90/0]_{2s}$ rectangular laminate plate with $a/b = 2$, $d/b = 0{\cdot}8$ and with two simply supported ends and two fixed ends is shown in Fig. 3(c).

Figure 9 shows the optimal fiber angle and the associated optimal buckling load versus plate aspect ratio for $[\pm\theta/90/0]_{2s}$ rectangular composite plates with a central circular cutout. From Fig. 9(a), we can

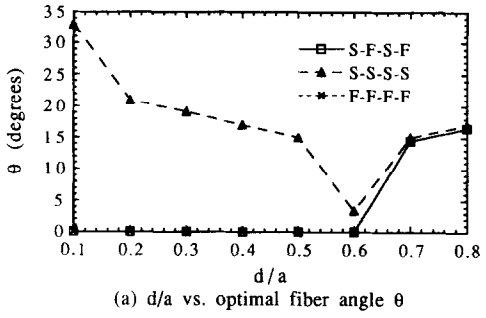

(a) d/a vs. optimal fiber angle θ

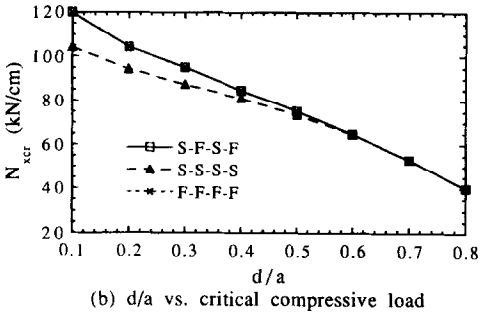

(b) d/a vs. critical compressive load

Fig. 8. Effect of end conditions and sizes of cutouts on buckling optimization of uniaxially compressed $[\pm\theta/90/0]_{10s}$ square composite plates with a central circular cutout.

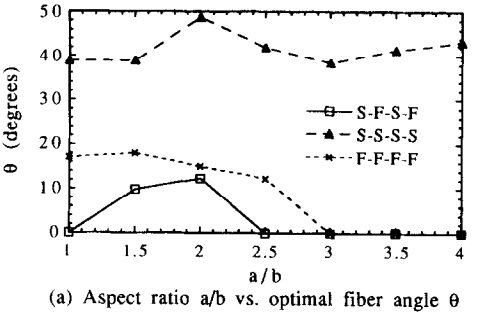

(a) Aspect ratio a/b vs. optimal fiber angle θ

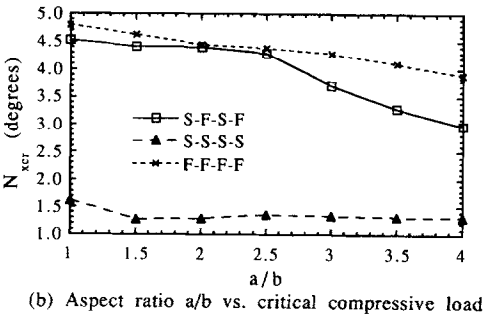

(b) Aspect ratio a/b vs. critical compressive load

Fig. 9. Effect of end conditions and plate aspect ratios on buckling optimization of uniaxially compressed $[\pm\theta/90/0]_{2s}$ rectangular composite plates with a central circular cutout $(d/b = 0{\cdot}8)$.

see that the optimal fiber angle for plates with four simply supported ends is greater than those of plates with other end conditions. The optimal fiber angles of plates with four fixed ends and plates with two simply supported ends and two fixed ends gradually approach 0° when the plate aspect ratios are large. Figure 9(b) shows that the optimal buckling loads for plates with four fixed ends, and with two simply supported ends and two fixed ends gradually decrease when the a/b ratio increases. It seems that the optimal buckling loads of plates with four simply supported ends are insensitive to the a/b ratio.

Figure 10 shows the optimal fiber angle θ and the associated optimal buckling load versus plate aspect ratio for $[\pm 0/90/0]_{10s}$ rectangular composite plates with a central circular cutout. We can see that the results of optimization (both optimal fiber angle and optimal buckling load) for these plates with various end conditions are very close. Comparing Fig. 10 with Fig. 9, we can observe that the results of optimization for thin plates with various end conditions are quite different. However, for thick plates, the end conditions have almost no influence on the results of optimization.

Comparing plates with cutouts (Fig. 9) with plates without cutouts (Fig. 4), we can see that the cutouts cause the results of optimization of thin plates with two simply supported ends and two fixed ends to be close to those of plates with four fixed ends. Comparing Fig. 10 with Fig. 5, we can see that the cutouts cause the results of optimization of thick plates with different end conditions to become close together.

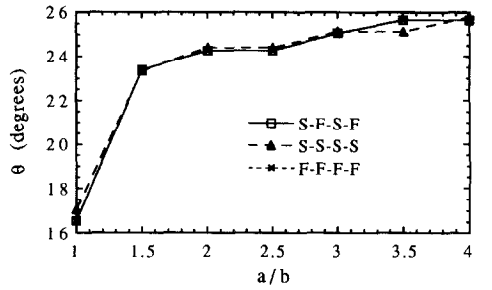

(a) Aspect ratio a/b vs. optimal fiber angle θ

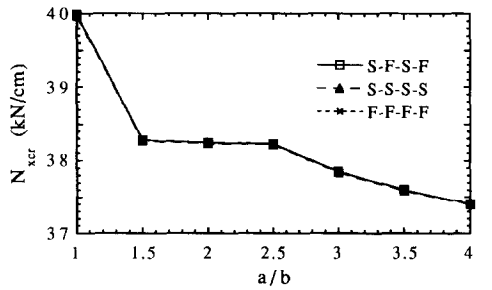

(b) Aspect ratio a/b vs. critical compressive load

Fig. 10. Effect of end conditions and plate aspect ratios on buckling optimization of uniaxially compressed $[\pm\theta/90/0]_{10s}$ rectangular composite plates with a central circular cutout $(d/b = 0{\cdot}8)$.

6 CONCLUSIONS

In the process of sequential linear programming, most optimal results are obtained within 11 iterations, and the results are all verified by choosing different initial guesses. Hence, as a general conclusion, the sequential linear programming is efficient and stable to solve non-linear optimization problems.

For the optimal buckling analysis of uniaxially compressed symmetrically laminated plates with various plate thicknesses, aspect ratios, circular cutouts and end conditions, the following conclusions may be drawn.

1. For thin rectangular composite plates without cutouts, and with various end conditions, the optimal fiber angles seem to vary around certain values when the plate aspect ratios are increased. For thick plates, the optimal fiber angles are sensitive to the end conditions even when the plate aspect ratios are large. When the plate aspect ratios are increased, the optimal buckling loads of all thin and thick plates with different end conditions gradually approach to constant values.
2. The optimal fiber angles and the optimal buckling loads of thin square composite plates with a central circular cutout are influenced significantly by the end conditions. The optimal buckling loads of these plates, except the plates with four simply supported ends, increase with the increase of the sizes of cutouts. Hence, it is possible to tailor the cutout size and fiber angle to increase the buckling loads of traction loaded plates beyond those of corresponding plates without cutouts.
3. For thick square composite plates with a central circular cutout, the results of optimization of plates with two simply supported ends and two fixed ends are the same as those of plates with four fixed ends. Nevertheless, when the sizes of the cutouts are large, the results of optimization for plates with different end conditions seem to be very close. In addition, the optimal buckling loads of these thick plates all decrease with the increase of the sizes of cutouts.
4. The presence of a central circular cutout for thin rectangular composite plates causes the results of optimization for plates with two simply supported ends and two fixed ends to be close to those of plates with four fixed ends.
5. The presence of a central circular cutout for thick rectangular composite plates causes the

end conditions to have almost no influence on the results of optimization.

In this paper, bifurcation buckling analysis is carried out based on the assumption that the composite laminate material behaves linearly. For low aspect ratio plates and for plates with large cutouts, the stresses in the laminates may exceed the elastic range and these laminates are probably driven by compression strength failure instead of buckling. In these cases, buckling analyses of composite plates based on non-linear material properties are recommended.[24]

REFERENCES

1. Crouzet-Pascal, J., Buckling analysis of laminated composite plates. *Fibre Sci. Technol.*, **11** (1978) 413–46.
2. Hirano, Y., Optimum design of laminated plates under axial compression. *AIAA J.*, **17** (1979) 1017–19.
3. Leissa, A. W., Buckling of laminated composite plates and shell panels. AFWAL-TR-85-3069, Flight Dynamics Laboratory, Wright-Patterson Air Force Base, OH, 1985.
4. Muc, A., Optimal fibre orientation for simply-supported angle-ply plates under biaxial compression. *Comp. Struct.*, **9** (1988) 161–72.
5. Rhodes, M. D., Mikulas, M. M. & McGowan, P. E., Effects of orthotropy and width on the compression strength of graphite–epoxy panels with holes. *AIAA J.*, **22** (1984) 1283–92.
6. Nemeth, M. P., Importance of anisotropy on buckling of compression-loaded symmetric composite plates. *AIAA J.*, **24** (1986) 1831–5.
7. Nemeth, M. P., Buckling behavior of compression-loaded symmetrically laminated angle-ply plates with holes. *AIAA J.*, **26** (1988) 330–6.
8. Vellaichamy, S., Prakash, B. G. & Brun, S., Optimum design of cutouts in laminated composite structures. *Computers Struct.*, **37** (1990) 241–6.
9. Schmit, L. A., Structural synthesis—its genesis and development. *AIAA J.*, **19** (1981) 1249–63.
10. Zienkiewicz, O. C. & Champbell, J. S., Shape optimization and sequential linear programming. In *Optimum Structural Design, Theory and Applications*, ed. R. H. Gallagher & O. C. Zienkiewicz. John Wiley, New York, 1973, pp. 109–26.
11. Vanderplaats, G. N., *Numerical Optimization Techniques for Engineering Design with Applications*, chapter 6. McGraw-Hill, New York, 1984.
12. Hibbitt, Karlsson and Sorensen Inc., *ABAQUS User and Theory Manuals*, Version 5.4. Providence, RI, 1995.
13. Wang, C. T., *Applied Elasticity*, chapter 9. McGraw-Hill, New York, 1953.
14. Chajes, A., *Principles of Structural Stability Theory*, chapter 1. Prentice-Hall, 1974.
15. Cook, R. D., Malkus, D. S. & Plesha, M. E., *Concepts and Applications of Finite Element Analysis*, 3rd edn, chapter 14. John Wiley, New York, 1989.
16. Bathe, K. J. & Wilson, E. L., Large eigenvalue problems in dynamic analysis. *J. Eng. Mech. Div. ASCE*, **98** (1972) 1471–85.
17. Irons, B. M., The semi-loof shell element. In *Finite Elements for Thin Shells and Curved Members*, ed. D. G. Ashwell & R. Gallagher. John Wiley, London, 1976, pp. 197–222.
18. Whitney, J. M., Shear correction factors for orthotropic laminates under static load. *J. Appl. Mech.*, **40** (1973) 302–4.
19. Kolman, B. & Beck, R. E., *Elementary Linear Programming with Applications*, chapter 2. Academic Press, Orlando, 1980.
20. Esping, B. J. D., Minimum weight design of membrane structures. *Computers Struct.*, **19** (1984) 707–16.
21. Crawley, E. F., The natural modes of graphite/epoxy cantilever plates and shells. *J. Comp. Mater.*, **13** (1979) 195–205.
22. Maror, M. J., *Numerical Analysis A Practical Approach*, 2nd edn, chapter 2. Macmillan, New York, 1987.
23. Ritchie, D. & Rhoades, J., Buckling and postbuckling behavior of plates with holes. *Aeronaut. Quart.*, **26** (1975) 281–96.
24. Hu, H.-T., Buckling analyses of fiber composite laminate shells with material nonlinearity. *J. Comp. Technol. Res.*, **15** (1993) 202–8.